science, engineering and health studies

Research Article

Science, Engineering and Health Studies
https://lio1.tci-thaijo.org/index.php/sehs
ISSN (Online): 2630-0087

Comparison between consumer-oriented and laboratory benchtop near-infrared spectrometers for total soluble solids measurement in grape

Pramote Khuwijitjaru[1], Parika Rungpichayapichet[1], and Christian W. Huck[2]*

[1] Department of Food Technology, Faculty of Engineering and Industrial Technology, Silpakorn University, Nakhon Pathom 73000, Thailand
[2] Institute of Analytical Chemistry and Radiochemistry, University of Innsbruck, 6020 Innsbruck, Austria

***Corresponding author**:
Pramote Khuwijitjaru
khuwijitjaru_p@su.ac.th

***Received**: 22 December 2023*
***Revised**: 6 February 2024*
***Accepted**: 9 March 2024*
***Published**: 14 November 2024*

***Citation**:
Khuwijitjaru, P., Rungpichayapichet, P., and Huck, C. W. (2024). Comparison between consumer-oriented and laboratory benchtop near-infrared spectrometers for total soluble solids measurement in grape. Science, Engineering and Health Studies, 18, 24030003.

ABSTRACT

Portable near-infrared (NIR) spectrometers are gaining interest as a non-destructive tool for fruit quality determination in the decade. In this study, the performance of the portable NIR spectrometer for TSS prediction of grapes was evaluated and compared to the benchtop spectrometer. A total of 105 table grapes were individually measured NIR spectra at short-wavelength (740 – 1070 nm) and long-wavelength NIR region (1000 – 2500 nm) using SCiO and NIRFlex N-500 spectrometers, respectively. Partial least square (PLS) regression analysis was performed on berry spectra from both devices afterward significant wavelengths were identified and used to develop multiple linear regression (MLR) models. The best PLS prediction model was obtained from SNV pretreating spectra for both devices and spectral data acquired from SCiO showed better prediction performance (R_V^2 = 0.854, SEP = 0.452°Brix) than NIRFlex N-500 spectra (R_V^2 = 0.667, SEP = 0.675°Brix). Low predicting ability was gained for the MLR calibration model for both device with an RPD of about 1.70. From the results, a pocket-size spectrometer has the potential to be a non-destructive sorting and screening tool in fruit industries.

Keywords: grape; NIR spectroscopy; portable; total soluble solids; partial least-square regression

1. INTRODUCTION

Near-infrared (NIR) spectroscopy is one of the rapid and/or non-destructive analytical methods employed in many fields of research and industries, particularly food and agriculture (Khuwijitjaru, 2018; Basile et al., 2022; Li et al., 2023). The technique relies on the selective absorption and reflection of an electromagnetic wave in the range of 800 – 2500 nm by the hydrogen-containing molecules in samples together with various chemometric methods for analyzing the spectrum data relating to the sample's chemical composition (Ye et al., 2023). The potential of NIR spectroscopy for fruit internal quality assessment has been widely reported. In particular, NIR spectroscopy has been successfully used to determine the total soluble solids (TSS) of various fruits such as mango (Sharma et al., 2020; Rungpichayapichet et al., 2023), apple (Guo et al., 2016; Pissard et al., 2021), pear (Li et al., 2019), strawberry (Agulheiro-Santos et al., 2022; Saad et al., 2022), and grapes (Costa et al., 2019; Chariskou et al., 2022; Ye et al., 2023).

For decades, the feasibility of using laboratory benchtop and portable or handheld NIR spectrometers to inspect the quality of agricultural products has been studied and the performance of the two instruments was compared. Due to the compact size and cost-effectiveness, portable or handheld NIR devices have become widespread in on-site or in-field measurement and online as process analytical technology (Donis-González et al., 2020; McVey et al., 2021; Pissard et al., 2021) Interestingly, recent NIR spectrometers are becoming much smaller due to the advancement of hardware development (Antila et al., 2013). For this reason, handheld NIR instruments are more widely available for businesses or even individual consumers.

SCiO (Consumer Physics Inc., Tel-Aviv, Israel), a small-size, consumer-oriented NIR spectrometer, has been commercialized in recent years. The instrument measures NIR in the range of 740 – 1070 nm, which is usually considered as a short-NIR range. Its performance has been investigated in some studies. The results, however, were inconsistent. Studies on measurements of antioxidant capacity in grains (Wiedemair and Huck, 2018), water, and fat contents in cheese (Wiedemair et al., 2019) showed promising results, while quantitative analysis of total soluble solids (TSS) in kiwifruit, apple, feijoa, and avocado was reported as unsuccessful (Li et al., 2018).

Donis-González et al. (2020) reported that the performance of the prediction model using spectral data from SCiO spectrometer to determine the TSS of grape and peach was lower than the prediction model using spectral data from a portable NIR spectrometer (F-750). Fair predicting ability on the coriander seed authenticity investigation was gained from a model using spectra from SCiO compared to benchtop and other portable NIR instruments (McVey et al., 2021). However, a few studies showed the potential of the SCiO spectrometer as a fast sorting and screening of TSS of wine grapes (Ferrara et al., 2022b) and table grapes (Ferrara et al., 2022a).

In this study, the potential of consumer-oriented and laboratory benchtop NIR spectrometers for TSS determination in grapes was compared.

2. EXPERIMENTAL

2.1 Raw material

Table grapes (Superior, Giovanni Grasso S.r.L., Italy) were purchased from a local supermarket in Innsbruck, Austria. A total of 105 fruits were used.

2.2 NIR spectra acquisition

First, the fruits were individually scanned with a SCiO sensor on the surface, and SCiO Lab, an online application on the smartphone, was used to collect absorbance data in the wavelength range of 740 – 1070 nm with a resolution less than 10 cm^{-1} and a sampling interval of 1 nm. After that, the fruit was scanned by NIRFlex N-500 equipped with a Fiber Optic Solids cell (BÜCHI Labortechnik AG, Flawil, Switzerland) in the long-wavelength range 4000 – 10,000 cm^{-1} (1000 – 2500 nm) with the resolution of 8 cm^{-1} and number of scans of 32. For both instruments, spectral measurement of each fruit was randomly done from 5 points on the fruit and the average value was calculated and represented as the fruit spectrum.

2.3 TSS measurement

TSS of each berry was determined using an Abbe refractometer (A.KRÜSS Optronic, Hamburg, Germany) with a temperature sensor. Grape juice was manually squeezed and dropped on the refractometer. The temperature during the measurement was recorded and used for correction according to Method OIV-MA-AS2-02 (OIV, 2012). Measurement was done in duplicate and expressed as °Brix.

2.4 Chemometric analysis

To avoid the difference of the specific software used by each instrument, spectral preprocessing and chemometric analysis were performed using The Unscrambler software (version 9.7, Camo, Oslo, Norway). Spectra acquired from NIRFlex N-500 in wavenumber were transformed to wavelength prior to preprocessing. Five different mathematical preprocessings of the spectra including Savitzky–Golay smoothing (SG), Savitzky–Golay first derivative (D), Savitzky–Golay second derivative (D^2) using 7 and 15 points with second-order polynomial regression, standard normal variate (SNV) transformation, and multiplicative scatter correction (MSC) were performed during the development of the calibration models to improve the prediction performance.

A total of 105 fruits were divided into calibration (79 samples) and test (26 samples) sets. TSS was sorted and the samples were selected by specific intervals 'Every 3 samples counting from 3' using The Unscrambler program, and the two highest and two lowest values were assigned to the calibration set. Firstly, calibration models were developed using partial least square (PLS) regression. Then, the specific wavelengths obtained from the relatively high absolute values in PLS regression coefficient plots and the loading weight plot of the best-fitting PLS model were selected and used to build multiple linear regression (MLR) models. Multifactorial analysis (backward elimination stepwise method) was applied to identify significant wavelengths. MLR calibration models were established using the same calibration and test set samples as PLS models. The goodness-of-fit of the prediction models was evaluated using the coefficient of determination (R_C^2) and standard error of calibration (SEC) and validation was evaluated based on the coefficient of prediction (R_V^2), standard error of prediction (SEP), bias, and the ratio of the standard deviation of the test set to SEP (RPD). The high-performance predictive model should have an R^2 close to 1.0, an RPD between 2.5 and 3.0, and a low SEP (Donis-González et al., 2020; Ferrara et al., 2022b). The difference between actual and predicted values obtained from prediction models was analyzed by paired t-tests (SPSS version 17, Chicago, IL, USA).

3. RESULTS AND DISCUSSION

3.1 Fruit quality

TSS is commonly used as a ripeness parameter of table grapes. According to maturity requirements in UNECE standard FFV-19 concerning the marketing and commercial quality control of table grapes, the TSS of matured grapes must be at least 16° Brix (UNECE, 2018). In this study, TSS ranged from 18.33 – 24.09°Brix which satisfied the maturity requirement. The majority (60% of total samples) of the TSS value of berry was found to be 20-22°Brix.

3.2 NIR spectra

The mean absorbance spectra of grapes at different ripeness levels obtained from both devices are shown in Figure 1. Spectra acquired from SCiO at the short-wavelength region (740-1070 nm) displayed a board band peak around 900-1050 nm. A high overlap and a very broad band peak were generally observed in the short-wavelength region due to the absorption at high overtone and combination bands (Chandrasekaran et al., 2019). The absorption peak around 900-1050 nm is related to the absorption of -OH groups in water and carbohydrates such as sugars and organic acid (Rungpichayapichet et al., 2016; Donis-González et al., 2020; Ping et al., 2023). Three overlapping peaks around 1100-1300, 1500-1600, and 1900-2100 nm that are associated with the absorption of -CH and -OH groups were observed in spectra collected from NIRFlex N-500. Similar characteristics, patterns, and shape of absorbance spectra were noticed whereas baseline shift was observed as a result of ripeness variation. High TSS berries showed higher NIR absorption than low TSS berries in the short-wavelength region while the contradiction results were found in the long-wavelength region. Because the overlapping and baseline shift effects were observed, several preprocessing techniques were applied to spectral data prior to calibration development to enhance the prediction performance of the model.

3.3 PLS calibration for predicting the TSS of table grapes

Table 1 shows the descriptive statistics of TSS of berries used in calibration and test sets. PLS regression results obtained for the original and preprocessing spectra of the SCiO spectrometer and NIRFlex N-500 spectrometer are presented in Table 2.

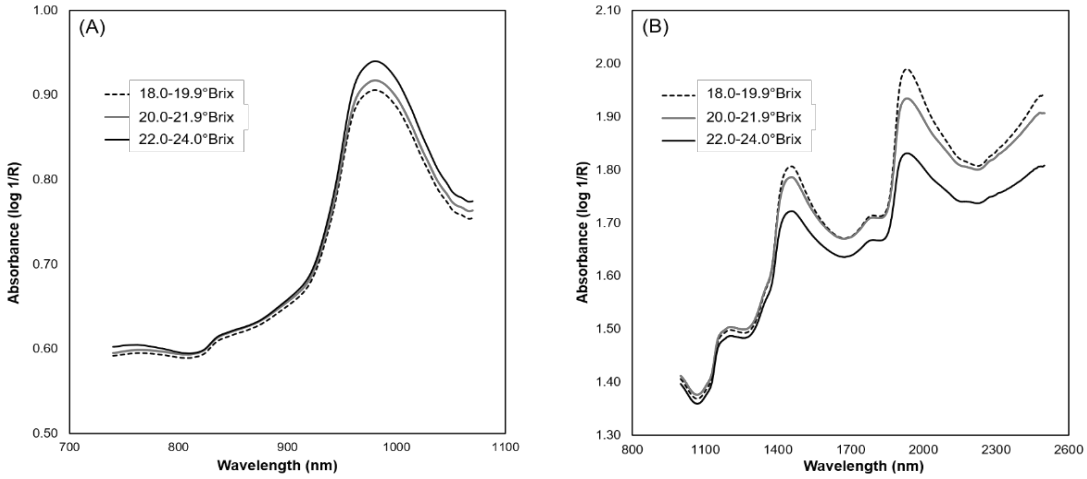

Figure 1. Average original spectra of grapes in different ripeness acquired by SCiO (A) at 740 – 1070 nm and NIRFlex N-500 (B) at 1000 – 2500 nm

Table 1. Descriptive statistic for the calibration and test sets for TSS prediction

	Calibration set	Test set
Number of samples	79	26
Maximum (°Brix)	24.09	23.84
Minimum (°Brix)	18.33	18.85
Mean (°Brix)	21.03	21.03
Standard deviation (°Brix)	1.19	1.19

For the TSS calibration models developed from the SCiO spectrometer, the R_V^2 ranged from 0.655 to 0.854 and SEP were between 0.452 - 0.696°Brix. A non-notable difference was found between PLS calibration models preprocessed with SNV and MSC techniques. The best predicting performance model was obtained from SNV pretreated spectra with R_V^2 , SEP, bias, and RPD of 0.85, 0.45°Brix, 0.03°Brix, and 2.63, respectively. The overall calibration results obtained from long-wavelength spectra showed lower prediction performance than the spectra acquired from short-wavelength regions. Regarding spectral preprocessing technique, SNV and MSC pretreated spectral data provided high prediction performance of the TSS calibration model for the NIRFlex N-500 spectrometer. The results were in agreement with other reports that pretreating spectral data with SNV and MSC techniques gave the best result for TSS prediction of grapes (Daniels et al., 2019; Donis-González et al., 2020; Kanchanomai et al., 2020; Ferrara et al., 2022b; Ping et al., 2023). This might be due to the baseline correction function of MSC and SNV which can minimize the effect of non-uniform light scattering (Daniels et al., 2019; Li et al., 2019). The TSS calibration model obtained from SCiO showed better prediction performance than that of NIRFlex N-500. This might be caused by the effect of light penetration. The high accuracy of the prediction model obtained from short-wavelength spectra might be attributed to the deeper light penetration depth of short-wavelength compared to long-wavelength regions (Li et al., 2018). As reported by Ferrara et al. (2022a) the light penetration depth of short-wavelength (700-900 nm) can be up to 4 mm while long-wavelength (900-1900 nm) is 2-3 mm; therefore, the

spectral data acquired from the short-wavelength region are more correlated with the chemical compositions in fruit pulp. Regarding RPD, the short-wavelength SNV pretreating spectra calibration model shows good prediction accuracy (RPD 2.63), whereas long-wavelength SNV pretreating spectra calibration can only distinguish between low and high values (RPD 1.76) (Daniels et al., 2019). Figure 2 illustrates the scatter plots of the best PLS calibration results obtained from short- and long-wavelength spectra. A non-significant difference was found between the TSS value predicted by both calibration models and the actual value ($p > 0.05$, paired t-test).

Table 2. PLS regression model results for TSS in grape

Quality attribute	Spectral preprocessing technique[a]	LVs	Calibration set		Prediction set			
			R_C^2	SEC	R_V^2	SEP	Bias	RPD
SCiO								
TSS (°Brix)	Original	8	0.86	0.45	0.83	0.48	0.08	2.48
	SG7	10	0.90	0.38	0.82	0.47	0.17	2.51
	SG15	8	0.87	0.44	0.82	0.49	0.13	2.43
	D7	3	0.75	0.59	0.81	0.51	0.05	2.33
	D15	5	0.84	0.48	0.72	0.63	-0.01	1.90
	D²7	5	0.83	0.49	0.66	0.70	-0.03	1.71
	D²15	5	0.84	0.48	0.72	0.63	-0.01	1.90
	SNV	**5**	**0.80**	**0.53**	**0.85**	**0.45**	**0.03**	**2.63**
	MSC	5	0.80	0.53	0.85	0.45	0.03	2.63
NIRFlex N-500								
TSS (°Brix)	Original	9	0.81	0.52	0.57	0.77	0.11	1.55
	SG7	6	0.72	0.64	0.57	0.77	-0.14	1.55
	SG15	6	0.71	0.64	0.57	0.77	-0.14	1.55
	D7	10	0.91	0.35	0.40	0.92	-0.09	1.30
	D15	9	0.89	0.41	0.66	0.69	-0.10	1.74
	D²7	10	0.93	0.33	0.08	1.20	-0.03	0.99
	D²15	1	0.29	1.01	0.12	1.19	-0.02	1.00
	SNV	**6**	**0.75**	**0.60**	**0.67**	**0.68**	**-0.12**	**1.76**
	MSC	6	0.74	0.61	0.67	0.67	-0.11	1.77

[a] SG7 = Smoothing using the Savitzky-Golay algorithm with 7 points average, SG15 = Smoothing using the Savitzky-Golay algorithm with 15 point average, D7 = First derivative using the Savitzky-Golay algorithm with 7 points average, D15 = First derivative using the Savitzky-Golay algorithm with 15 points average, D²7 = Second derivative using the Savitzky-Golay algorithm with 7 points average, D²15 = Second derivative using the Savitzky-Golay algorithm with 15 points average, SNV = Standard Normal Variate, MSC = Multiplicative Scattering Correction. Bold figures indicate best predicting performance models.

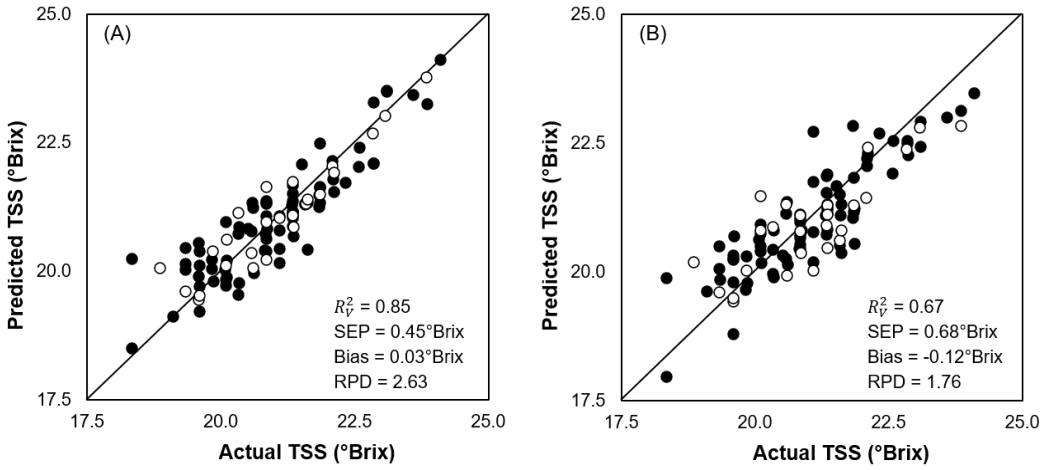

Figure 2. Prediction results of TSS of grape using PLS calibration model established from the spectral data obtained from SCiO spectrometer (A) and NIRFlex N-500 spectrometer (B). (● is calibration set and ○ is test set)

3.4 MLR calibration for predicting TSS of table grapes

Significant wavelength selection was done by using multifactorial analysis (backward elimination stepwise method). First, wavelengths with the highest regression coefficients (absolute value) in the PLS model were selected as the candidate wavelengths. Then, multifactorial analysis was used to evaluate the significance of each wavelength (Walczak and Massart, 2000). In each run, non-significant wavelengths were removed and the MLR calibration was re-established until only significant wavelengths were left in the model. Regarding regression coefficient plots of PLS calibration from both devices, thirteen candidate wavelengths were chosen and were subjected to multifactorial analysis with a backward elimination stepwise method. Five significant wavelengths (811, 836, 914, 955, and 1008 nm) were obtained for the MLR calibration model developed from SCiO spectral data and the MLR calibration model of NIRFlex N-500 spectra (1395, 1460, 2034, 2134, and 2312 nm) (Figure 3). A similar group of significant wavelengths for the TSS prediction model of grape were reported. Ping et al. (2023) used the competitive adaptive weighting algorithm to define effective wavelengths for the prediction of TSS of table grape and found that there were 53 significant wavelengths which included 836, 910, 958, 1391, and 1468 nm in one group. Li et al. (2019) reported that a group of sugar-related wavelengths included the O-H combination band at 840 nm, and the third overtone of C-H and O-H stretching at 910 nm and 950 nm, respectively. Therefore, significant wavelengths were used to establish the MLR calibration model.

MLR models for predicting TSS of grapes using SNV pretreated spectral data obtained from SCiO spectrometer and NIRFlex N-500 spectrometer are shown in Equations (1) and (2), respectively.

Prediction results of TSS of grape using the MLR calibration models are shown in Figure 4. A comparable predicting performance model was noticed for MLR and PLS calibration using long-wavelength spectra, whereas the MLR calibration obtained using short-wavelength spectra showed less prediction performance. Similar results showed that using a smaller number of variables in the prediction model provided slightly less accuracy than the model obtained from full-range spectra (Fernández-Novales et al., 2009; Costa et al., 2019). However, a non-significant difference was found between the TSS value predicted by the MLR calibration model obtained from both spectral range and actual value ($p > 0.05$, paired t-test).

$$\text{TSS (°Brix)} = -59.8 + 87.2 \cdot \lambda_{811} - 167.2 \cdot \lambda_{836} + 40.9 \cdot \lambda_{914} - 27.6 \cdot \lambda_{955} + 53.1 \cdot \lambda_{1008} \quad (1)$$

$$\text{TSS (°Brix)} = 70.5 - 36.9 \cdot \lambda_{1395} + 21.6 \cdot \lambda_{1460} - 48.6 \cdot \lambda_{2034} + 25.3 \cdot \lambda_{2134} - 13.9 \cdot \lambda_{2312} \quad (2)$$

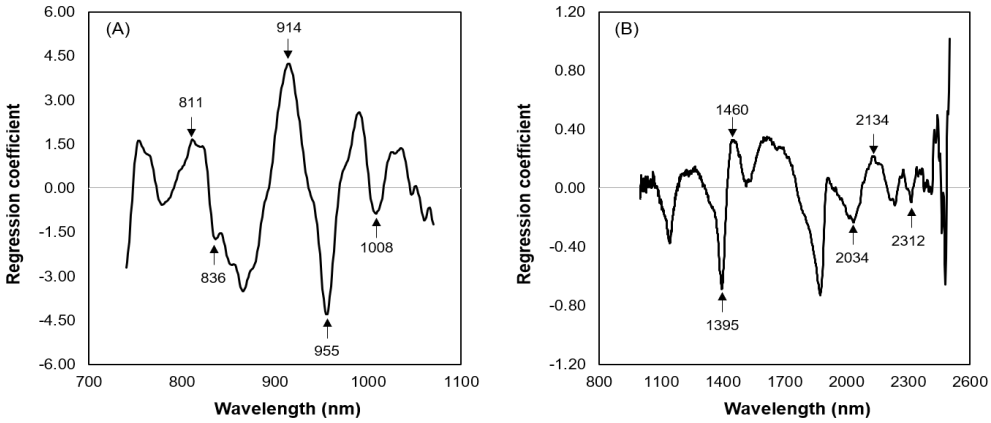

Figure 3. PLS regression coefficient plot showing significant wavelengths used for MLR calibration prediction model for SciO spectrometer (A) and NIRFlex N-500 spectrometer (B)

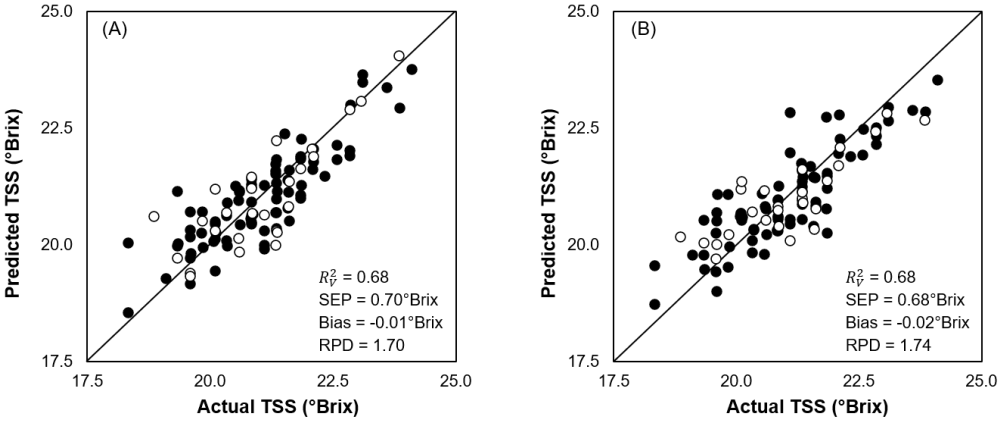

Figure 4. Prediction results of TSS of grape using MLR calibration model established from the spectral data obtained from SCiO spectrometer (A) and NIRFlex N-500 spectrometer (B). (● is calibration set and ○ is test set)

4. CONCLUSION

The results of this study showed the potential of the SCiO sensor together with chemometric method to determine TSS in intact table grapes. For the PLS regression model, the calibration model developed from SCiO spectral data provided good prediction performance with a coefficient of determination (R_V^2), standard error of prediction (SEP) and the ratio of the standard deviation of the test set to SEP (RPD) about 0.854, 0.452°Brix and 2.63, respectively while fairly good prediction performance (R_V^2 = 0.667, SEP =0.675°Brix and RPD = 1.76) was gained from NIR benchtop spectral data. The backward elimination stepwise method was used to define the significant wavelengths for MLR calibrations. Less accuracy was found for the MLR prediction model due to the minimum number of variables. However, the calibration models performed reasonably well for the sorting and screening of grapes. Therefore, a small NIR sensor can support grape and wine production as a rapid and non-destructive tool for grape quality assessment.

ACKNOWLEDGMENT

P. Khuwijitjaru gratefully acknowledges the ASEA-UNINET Staff Exchange, One Month Scholarship supported by Austrian Agency for International Cooperation in Education and Research (OeAD) and the Office of the Higher Education Commission (OHEC), Thailand.

REFERENCES

Agulheiro-Santos, A. C., Ricardo-Rodrigues, S., Laranjo, M., Melgão, C., and Velázquez, R. (2022). Non-destructive prediction of total soluble solids in strawberry using near infrared spectroscopy. *Journal of the Science of Food and Agriculture*, 102(11), 4866–4872.

Antila, J., Tuohiniemi, M., Rissanen, A., Kantojärvi, U., Lahti, M., Viherkanto, K., Kaarre, M., and Malinen, J. (2013). MEMS- and MOEMS-based near-infrared spectrometers. In *Encyclopedia of Analytical Chemistry* (Meyers, R. A., Ed.). New Jersey: John Wiley & Sons.

Basile, T., Marsico, A. D., and Perniola, R. (2022). Use of artificial neural networks and NIR spectroscopy for non-destructive grape texture prediction. *Foods*, 11(3), 281.

Chandrasekaran, I., Panigrahi, S. S., Ravikanth, L., and Singh, C. B. (2019). Potential of near-infrared (NIR) spectroscopy and hyperspectral imaging for quality and safety assessment of fruits: An overview. *Food Analytical Methods*, 12(11), 2438–2458.

Chariskou, C., Vrochidou, E., Daniels, A. J., and Kaburlasos, V. G. (2022). Variable selection on reflectance NIR spectra for the prediction of TSS in intact berries of Thompson seedless grapes. *Agronomy*, 12(9), 2113.

Daniels, A. J., Poblete-Echeverria, C., Opara, U. L., and Nieuwoudt, H. H. (2019). Measuring internal maturity parameters contactless on intact table grape bunches using NIR spectroscopy. *Frontiers in Plant Science*, 10, 1517.

Donis-González, I. R., Valero, C., Momin, M. A., Kaur, A., and Slaughter, D. C. (2020). Performance evaluation of two commercially available portable spectrometers to non-invasively determine table grape and peach quality attributes. *Agronomy*, 10(1), 148.

dos Santos Costa, D., Mesa, N. F. O., Freire, M. S., Ramos, R. P., and Mederos, B. J. T. (2019). Development of predictive models for quality and maturation stage attributes of wine grapes using vis-nir reflectance spectroscopy. *Postharvest Biology and Technology*, 150, 166–178.

Fernández-Novales, J., López, M.-I., Sánchez, M.-T., Morales, J., and González-Caballero, V. (2009). Shortwave-near infrared spectroscopy for determination of reducing sugar content during grape ripening, winemaking, and aging of white and red wines. *Food Research International*, 42(2), 285–291.

Ferrara, G., Marcotuli, V., Didonna, A., Stellacci, A. M., Palasciano, M., and Mazzeo, A. (2022a). Ripeness prediction in table grape cultivars by using a portable NIR device. *Horticulturae*, 8(7), 613.

Ferrara, G., Melle, A., Marcotuli, V., Botturi, D., Fawole, O. A., and Mazzeo, A. (2022b). The prediction of ripening parameters in Primitivo wine grape cultivar using a portable NIR device. *Journal of Food Composition and Analysis*, 114, 104836.

Guo, Z., Huang, W., Peng, Y., Chen, Q., Ouyang, Q., and Zhao, J. (2016). Color compensation and comparison of shortwave near infrared and long wave near infrared spectroscopy for determination of soluble solids content of 'Fuji' apple. *Postharvest Biology and Technology*, 115, 81–90.

Kanchanomai, C., Ohashi, S., Naphrom, D., Nemoto, W., Maniwara, P., and Nakano, K. (2020). Non-destructive analysis of Japanese table grape qualities using near-infrared spectroscopy. *Horticulture, Environment, and Biotechnology*, 61(4), 725–733.

Khuwijitjaru, P. (2018). Near infrared spectroscopy research performance in food science and technology. *NIR News*, 29(3), 12–14.

Li, J., Wang, Q., Xu, L., Tian, X., Xia, Y., and Fan, S. (2019). Comparison and optimization of models for determination of sugar content in pear by portable Vis-NIR spectroscopy coupled with wavelength selection algorithm. *Food Analytical Methods*, 12, 12–22.

Li, L., Hu, D.-Y., Tang, T.-Y., and Tang, Y.-L. (2023). Non-destructive detection of the quality attributes of fruits by visible-near infrared spectroscopy. *Journal of Food Measurement and Characterization*, 17(2), 1526–1534.

Li, M., Qian, Z., Shi, B., Medlicott, J., and East, A. (2018). Evaluating the performance of a consumer scale SCiO™ molecular sensor to predict quality of horticultural products. *Postharvest Biology and Technology*, 145, 183–192.

McVey, C., Gordon, U., Haughey, S. A., and Elliott, C. T. (2021). Assessment of the analytical performance of three near-infrared spectroscopy instruments (benchtop, handheld and portable) through the investigation of coriander seed authenticity. *Foods*, 10(5), 956.

OIV (2012). *Compendium of International Methods of Wine and Must Analysis*, Paris: International Organisation of Vine and Wine.

Ping, F., Yang, J., Zhou, X., Su, Y., Ju, Y., Fang, Y., Bai, X., and Liu, W. (2023). Quality assessment and ripeness prediction of table grapes using visible–near-infrared spectroscopy, *Foods*, 12(12), 2364.

Pissard, A., Marques, E. J. N., Dardenne, P., Lateur, M., Pasquini, C., Pimentel, M. F., Pierna, J. A. F., and Baeten, V. (2021). Evaluation of a handheld ultra-compact

NIR spectrometer for rapid and non-destructive determination of apple fruit quality. *Postharvest Biology and Technology*, 172, 111375.

Rungpichayapichet, P., Chaiyarattanachote, N., Khuwijitjaru, P., Nakagawa, K., Nagle, M., Müller, J., and Mahayothee, B. (2023). Comparison of near-infrared spectroscopy and hyperspectral imaging for internal quality determination of 'Nam Dok Mai mango' during ripening. *Journal of Food Measurement and Characterization*, 17(2), 1501–1514.

Rungpichayapichet, P., Mahayothee, B., Nagle, M., Khuwijitjaru, P., and Müller, J. (2016). Robust NIRS models for non-destructive prediction of postharvest fruit ripeness and quality in mango. *Postharvest Biology and Technology*, 111, 31–40.

Saad, A. G., Azam, M. M., and Amer, B. M. A. (2022). Quality analysis prediction and discriminating strawberry maturity with a hand-held vis-NIR spectrometer. *Food Analytical Methods*, 15(3), 689–699.

Sharma, S., Sirisomboon, P., and Pornchaloempong, P. (2020). Application of a Vis-NIR spectroscopic technique to measure the total soluble solids content of intact mangoes in motion on a belt conveyor. *The Horticulture Journal*, 89(5), 545–552.

UNECE. (2018). *UNECE Standard FFV-19 Concerning the Marketing and Commercial Quality Control of Table Grapes*, Geneva: United Nations.

Walczak, B., and Massart, D. L. (2000). Calibration in wavelet domain. In *Data Handling in Science and Technology: Wavelets in Chemistry* (Walczak, B., Ed.), pp. 323–349. Amsterdam: Elsevier.

Wiedemair, V., and Huck, C. W. (2018). Evaluation of the performance of three hand-held near-infrared spectrometer through investigation of total antioxidant capacity in gluten-free grains. *Talanta*, 189, 233–240.

Wiedemair, V., Langore, D., Garsleitner, R., Dillinger, K., and Huck, C. (2019). Investigations into the performance of a novel pocket-sized near-infrared spectrometer for cheese analysis. *Molecules*, 24(3), 428.

Ye, W., Xu, W., Yan, T., Yan, J., Gao, P., and Zhang, C. (2023). Application of near-infrared spectroscopy and hyperspectral imaging combined with machine learning algorithms for quality inspection of grape: A review. *Foods*, 12(1), 132.